Excitation Spectra of Disordered Dimer Magnets Near Quantum Criticality

Matthias Vojta

Institut für Theoretische Physik, Technische Universität Dresden, 01062 Dresden, Germany

(Received 23 January 2013; revised manuscript received 16 August 2013; published 27 August 2013)

For coupled-dimer magnets with quenched disorder, we introduce a generalization of the bond-operator method, appropriate to describe both singlet and magnetically ordered phases. This allows for a numerical calculation of the magnetic excitations at all energies across the phase diagram, including the strongly inhomogeneous Griffiths regime near quantum criticality. We apply the method to the bilayer Heisenberg model with bond randomness and characterize both the broadening of excitations and the transfer of spectral weight induced by disorder. Inside the antiferromagnetic phase this model features the remarkable combination of sharp magnetic Bragg peaks and broad magnons, the latter arising from the tendency to localization of low-energy excitations.

DOI: 10.1103/PhysRevLett.111.097202 PACS numbers: 75.10.−b, 74.20.Mn, 74.72.−h, 75.45.+j

Magnetic quantum phase transitions (QPTs) have attracted enormous interest over the past two decades, with intriguing aspects such as Bose-Einstein condensation of magnons, exotic criticality, and non-Fermi-liquid behavior [1–4]. The influence of quenched disorder, being inevitable in condensed-matter systems, on QPTs is a less explored field, although a number of theoretical results are available [5,6]: disorder can modify the critical behavior or even destroy the QPT; in addition, it can produce singular response in off-critical systems via quantum Griffiths physics dominated by rare regions [7].

While the thermodynamics of disordered model systems near quantum criticality has been studied using a variety of theoretical tools [5], rather little is known about the dynamics of excitations in this fascinating regime, mainly because numerical methods are either restricted to the ground state or work in imaginary time where real-frequency spectra are difficult to extract, whereas analytical methods are restricted to low energy and to the limits of either weak or strong disorder. For quantum magnets, this issue is pressing, as high-resolution inelastic neutron scattering (INS) experiments are getting access to magnetic excitations near QPTs [8–11], and suitable materials with disorder created via intentional doping are available [12–15].

The aim of this Letter is to close this gap: for coupled-dimer magnets, being paradigmatic model systems for magnetic QPTs [1–3], we propose a generalization of the bond-operator method [16] to cases with quenched disorder. This enables the numerical calculation of magnetic excitation spectra in both paramagnetic and magnetically ordered phases, including the vicinity of the QPT, with disorder being treated exactly in finite-size systems. We apply the method to the square-lattice bilayer Heisenberg model, studied in detail in the disorder-free case [17–22], with different types of exchange randomness. Near quantum criticality, we generically find a strong broadening in both energy and momentum of the low-energy response, whereas that at high energy is less affected by disorder. An interesting dichotomy follows upon slightly moving into the antiferromagnetic (AFM) phase: the strongly inhomogeneous AFM features low-energy magnons that are distinctly broadened due to disorder-driven mode localization, but at the same time displays sharp Bragg peaks in its elastic response. We discuss connections to recent INS experiments.

Model.—We consider a Heisenberg magnet of coupled pairs of spins 1/2, with the general Hamiltonian

$$\mathcal{H} = \sum_i J_i \vec{S}_{i1} \cdot \vec{S}_{i2} + \sum_{\langle ii' \rangle mm'} K_{ii'}^{mm'} \vec{S}_{im} \cdot \vec{S}_{i'm'} \qquad (1)$$

defined on a lattice of N dimer sites i; J and K are the intradimer and interdimer couplings, and $m = 1, 2$ labels the two spins of each dimer. Without quenched disorder in the couplings J and K, this Hamiltonian can describe, e.g., spin ladders and bilayer Heisenberg magnets, but also applies to materials such as $TlCuCl_3$ [8,10,23–26] and $BaCuSi_2O_6$ [27–29].

Generalized bond-operator method.—Let the four states of each dimer i be $|t_k\rangle_i$, $k = 0, \ldots, 3$, where $|t_0\rangle = (|\uparrow\downarrow\rangle - |\downarrow\uparrow\rangle)/\sqrt{2}$, $|t_1\rangle = (-|\uparrow\uparrow\rangle + |\downarrow\downarrow\rangle)/\sqrt{2}$, $|t_2\rangle = i(|\uparrow\uparrow\rangle + \downarrow\downarrow\rangle)/\sqrt{2}$, $|t_3\rangle = (|\uparrow\downarrow\rangle + |\downarrow\uparrow\rangle)/\sqrt{2}$. Formally, bosonic operators $t_{ik}^\dagger$ can be introduced that create these states out of a fictitious vacuum, $|t_k\rangle_i = t_{ik}^\dagger |\mathrm{vac}\rangle_i$, with the constraint $\sum_k t_{ik}^\dagger t_{ik} = 1$ defining the physical Hilbert space [16]. In a paramagnetic phase, it is convenient to fully "condense" the singlet, such that the operators $t_{i\alpha}^\dagger$ ($\alpha = 1, 2, 3$) now create triplet excitations ("triplons") from a singlet background, and the constraint becomes of hard-core type $\sum_\alpha t_{i\alpha}^\dagger t_{i\alpha} \leq 1$ [21]. Approximations can then be understood as expansion about the singlet product state $|\psi_0\rangle = \prod_i |t_0\rangle_i$.

Magnetically ordered phases correspond to a condensate of triplets, such that the reference state now involves a linear combination of singlet and triplets on each site. A consistent description of excitations requires a basis rotation in the four-dimensional Hilbert space spanned by

the $|t_k\rangle$ [30,31]. Here, we generalize the approach of Ref. [30] to inhomogeneous states. For every dimer site, we introduce a SU(4) rotation to new basis states

$$|\tilde{t}_k\rangle_i = U^{(i)}_{kk'}|t_{k'}\rangle_i, \qquad \tilde{t}^\dagger_{ik} = U^{(i)}_{kk'}t^\dagger_{ik'} \qquad (k, k' = 0, \ldots, 3) \tag{2}$$

such that $|\tilde{\psi}_0\rangle = \prod_i |\tilde{t}_0\rangle_i$ replaces $|\psi_0\rangle$ as the reference state. For instance, $|\tilde{t}_0\rangle = (|t_0\rangle + |t_3\rangle)/\sqrt{2} = |\uparrow\downarrow\rangle$ describes a Néel state polarized along z. The $U^{(i)}$ are chosen such that $|\tilde{\psi}_0\rangle$ is the best product-state (i.e., saddle-point) approximation to the ground state of $\mathcal{H}$ (Supplemental Material [32]).

One now rewrites the Hamiltonian Eq. (1) in terms of the $|\tilde{t}_k\rangle_i$ using the transformation Eq. (2) (Supplemental Material [32]). In analogy to the paramagnetic case, one condenses $\tilde{t}^\dagger_0$, such that the $\tilde{t}^\dagger_\alpha$ ($\alpha = 1, 2, 3$) describe excitations on top of the reference state $|\tilde{\psi}_0\rangle$. The Hamiltonian takes the form $\mathcal{H} = \mathcal{H}_0 + \mathcal{H}_1 + \mathcal{H}_2 + \mathcal{H}_3 + \mathcal{H}_4$, where $\mathcal{H}_n$ contains n $\tilde{t}^{(\dagger)}_\alpha$ operators, and an additional hard-core constraint for the $\tilde{t}_\alpha$ is implied. With the proper (saddle-point) choice of the reference state, $\mathcal{H}_1$ vanishes, and $\mathcal{H}_2$ describes Gaussian fluctuations around an inhomogeneous magnetic state. $\mathcal{H}_2$ has the form

$$\mathcal{H}_2 = \sum_{ij\alpha\beta}\left[A^{\alpha\beta}_{ij}\tilde{t}^\dagger_{i\alpha}\tilde{t}_{j\beta} + \left(\frac{B^{\alpha\beta}_{ij}}{2}\tilde{t}_{i\alpha}\tilde{t}_{j\beta} + H.c.\right)\right] \tag{3}$$

where quenched disorder enters via random $A^{\alpha\beta}_{ij}$, $B^{\alpha\beta}_{ij}$. $\mathcal{H}_2$ is solved by a bosonic Bogoliubov transformation, which yields the $3N$ positive-energy eigenmodes of $\mathcal{H}_2$, used to calculate the dynamic spin susceptibility (Supplemental Material [32]). In both paramagnetic and collinearly ordered phases, the polarization directions decouple, giving rise to triply degenerate modes in the paramagnetic case and a longitudinal and two transverse modes in the collinear case.

The excitations described by this method interpolate continuously between triplons of a paramagnet and spin waves of a semiclassical AFM phase [30,33]. The present harmonic approximation constitutes the leading-order correction to $|\tilde{\psi}_0\rangle$ in a systematic expansion in $1/z$ with z the number of neighbors (Supplemental Material [32]) [34]. Anharmonic effects are neglected at this level; near criticality, this is qualitatively permissible if the anomalous exponent η is small [$\eta = 0.03$ for the Heisenberg model in (2 + 1) dimensions]. Their quantitative effect on the dispersion can be captured via a renormalization of model parameters [35]; below, we account for this by specifying parameters relative to the location of the QPT.

Bilayer magnet.—In the remainder of the Letter, we illustrate the application of the method to a simple case, namely, the bilayer Heisenberg model as realized, e.g., in $BaCuSi_2O_6$ [27–29]. Here, the dimers live on a two-dimensional (2D) square lattice with interlayer coupling J and intralayer coupling $K = K^{11}_{ii'} = K^{22}_{ii'}$ for nearest-neighbor sites i, i'. In the absence of disorder, this model is in a singlet ground state for $J \gg K$ and an AFM ground state with ordering wave vector $\vec{Q} = (\pi, \pi)$ for $J \ll K$, with an O(3) critical point at $(J/K)_c = 2.5220(1)$ [22]. In the harmonic bond-operator approach, this transition occurs at $(J/K)_c = 4$; including triplon interactions allows one to obtain a value very close to the exact result [21].

With disorder of random-mass type, the character of the QPT changes, as dictated by the Harris criterion [36]. Numerical simulations have shown that a new critical point with conventional power-law singularities emerges [37] for not too strong disorder [38]. Here, we shall focus on the excitation spectrum in the vicinity of this QPT upon inclusion of disorder where signatures of quantum Griffiths behavior can be expected [5,6].

Modeling disorder.—We shall mainly employ bimodal distributions of coupling constants, being experimentally relevant to cases where chemical substitution modifies exchange paths as occurs, e.g., in $Tl_{1-x}K_xCuCl_3$ [39] or $(C_4H_{12}N_2)Cu_2(Cl_{1-x}Br_x)_6$ [14]. Provided that all couplings remain AFM, this type of bond randomness does not introduce frustration, such that the magnetic order realized for $J \ll K$ continues to be collinear with wave vector $\vec{Q} = (\pi, \pi)$. We will denote the corresponding order parameter, the staggered magnetization per spin, by M_s.

Results: weak intradimer bonds and evolution across QPT.—We now present numerical results of our approach, for disordered intradimer coupling J, with values J_1 and J_2 taken with probabilities $(1 - p)$ and p, respectively, and use the interdimer coupling K as a tuning parameter to access the transition. Energies will be quoted in units of J_1, the system size is $N = L^2$ with $L = 64$ and additional 2^2 supercells, disorder averages are performed over $N_r = 50$ realizations, and the temperature is $T = 0$.

Results for small concentrations p of weak intradimer bonds, $J_2 = J_1/2$, are in Fig. 1: Figs. 1(a) and 1(b) display M_s as function of K and p, whereas Figs. 1(c)–1(h) show the dynamical susceptibility $\chi''(\vec{q}, \omega)$ for different parameter sets. This type of substitution drives the system towards the ordered phase by decreasing the apparent gap and shifting the QPT to smaller K value upon increasing p. There is a broad range of parameters with weak magnetic order, i.e., small nonzero M_s, to be discussed below.

Introducing a small amount p of disorder into the paramagnetic clean system causes a transfer of spectral weight to low energies [Figs. 1(c), 1(f)–1(h), and 2]. Doping creates excitations inside the gap that eventually induce weak order upon increasing p. This disorder-induced low-energy response, although centered around the ordering wave vector $\vec{Q}$, is broad in both momentum and energy (except for Goldstone modes at extremely small ω): this reflects the localization tendency of the corresponding modes (see Fig. 3). For intermediate p values near $1/2$, the spectrum visibly separates into upper and lower branches, which

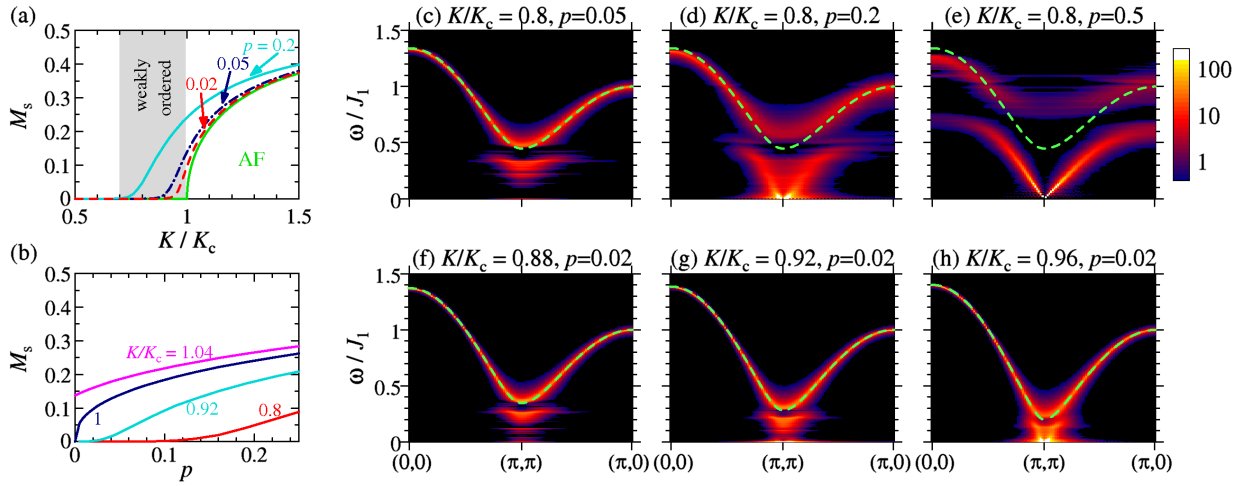

FIG. 1 (color online). Numerical results for the disordered bilayer Heisenberg model, with a concentration of p weak interlayer couplings with $J_2 = J_1/2$. (a) Phase diagram, showing the staggered magnetization M_s as function of K/K_c for different levels of disorder p, with $K_c = J_1/4$ denoting the critical coupling of the clean system in the linearized bond-operator approach. A regime with weak and strongly inhomogeneous order emerges for small p and $K \lesssim K_c$. (b) M_s as function of doping level p for different K values. [(c)–(h)] Transverse dynamic susceptibility $\chi''(\vec{q}, \omega)$ along a path in the 2D Brillouin zone ($q_z = \pi$) for different combinations of K/K_c and p. The green dashed lines indicate the dispersion of the clean system with the respective K.

exist over the entire Brillouin zone [Fig. 1(e)]; these branches correspond to modes that are primarily carried by either the J_1 or the J_2 intradimer bonds.

We now turn to a detailed analysis of the weak substitution-induced magnetic order. Figure 3 portraits a single realization of disorder by showing the spatial distribution of J and the local magnetization M_i as well as the wave functions for selected eigenmodes of $\mathcal{H}_2$. Several features are apparent: (i) The system develops islands of nonzero staggered magnetization [Fig. 3(b)] with a characteristic length scale of ξ, the correlation length of the clean reference system. These islands, being rare events in the sense of Griffiths [7], exist in regions with a greater concentration of weak interlayer bonds. (ii) The distribution of local magnetization values becomes broad on logarithmic scales [Fig. 3(f)], a typical fingerprint of Griffiths behavior. (iii) The low-energy "magnon" modes appear strongly localized on individual magnetization islands [Figs. 3(c) and 3(d)]. This behavior persists for essentially all energies below the gap of the clean reference system, whereas higher-energy modes tend to be delocalized [Fig. 3(e)]. We have confirmed this localization tendency by analyzing the inverse participation ratio (Supplemental Material [32]).

Taken together, this implies an interesting "dual" nature of the weakly ordered phase: It displays a sharp Bragg peak in the static structure factor $S(\vec{q})$ at $\vec{Q} = (\pi, \pi)$ [Fig. 4(a)] as the underlying order is perfectly staggered (albeit strongly inhomogeneous). At the same time, the small-ω

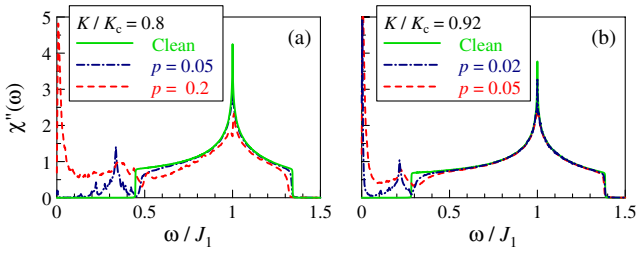

FIG. 2 (color online). Momentum-integrated transverse susceptibility $\chi''(\omega)$, for the bilayer model with random weak interlayer couplings as in Fig. 1. Disorder tends to close the spin gap by the transfer of spectral weight to low energies.

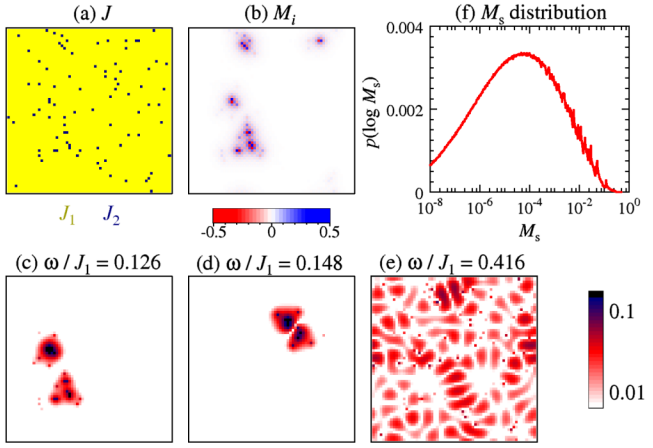

FIG. 3 (color online). Bilayer Heisenberg magnet with $K/K_c = 0.92$ and a single disorder realization of $p = 0.02$ weak intradimer bonds with $J_2 = J_1/2$, as in Fig. 1(g), with $L = 64$. (a) Spatial distribution of J values, indicating the location of the weak bonds. (b) Corresponding spatial distribution of the local magnetization M_i. [(c)–(e)] Wave function amplitudes of selected eigenmodes of $\mathcal{H}_2$. (f) Disorder-averaged probability distribution of local (staggered) magnetization values for parameters as in (a)–(e).

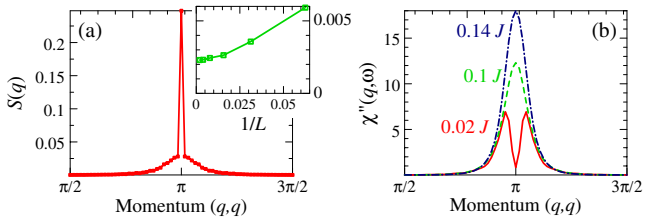

FIG. 4 (color online). (a) Static structure factor $S(\vec{q})$ and (b) susceptibility $\chi''(\vec{q}, \omega)$ at different ω values, for $K/K_c = 0.92$ and $p = 0.02$ weak intradimer bonds for $L = 128$. The inset in (a) shows the finite-size scaling of $[S(\vec{Q})/(2N)]^{1/2}$, which equals the order parameter M_s in the thermodynamic limit.

dynamic response $\chi''(\vec{q}, \omega)$ is anomalously broad in q space, due to the disorder-induced mode localization. This is shown in Fig. 4(b), where a spin-wave-like two-peak structure is only visible for extremely small $\omega/J \lesssim 0.02$.

Related localization and broadening phenomena have been observed and discussed both theoretically and experimentally for a variety of random magnets, mainly inside magnetically ordered [40–46] or quantum-disordered phases [47,48]. Our results show that, due to Griffiths physics, low-energy localization tendencies are significantly stronger near quantum criticality than those deep inside stable phases; for an extended discussion, see the Supplemental Material [32].

Further results.—We have studied other types of disorder, with selected results in Fig. 5 and the Supplemental Material [32]. Depending on the type of disorder, the overall triplon bandwidth may either increase or decrease with doping; the same applies to the apparent gap in $\chi''(\omega)$. For example, few *strong* intradimer bonds decrease the width of the main band (Fig. 5) because coherent triplon hopping is preempted through the strong bonds. Band splitting such as that in Fig. 1(e) is visible for sizeable bimodal disorder; for continuous distributions this is replaced by strong smearing of intensity. Most importantly, spectral broadening at low energies appears generic near the QPT; this effect is strongest if the dopants tend to drive the system towards the ordered phase, as in Fig. 1.

We have also performed calculations for other 2D unfrustrated coupled-dimer models, with qualitatively similar results, which thus appear generic.

Comparison to experiments.—Recent experiments [12,13,15] have studied bond randomness by ligand doping in spin-ladder materials. INS shows excitations with a greater energy width and an increased spin gap as compared to those of the undoped case. This consistent with our results for dopants that create locally stronger intradimer couplings, as in Fig. 5, or weaker interdimer couplings or both. For the investigated materials, such properties can indeed be deduced from studies of the end members of the doping series (Supplemental Material [32]).

Whereas INS data of bond-disordered nearly critical dimer magnets in 2D or 3D are not available to our knowledge, it is interesting to connect our results to $La_{2-x}Sr_xCuO_4$: at $x = 0.145$ this compound displays a field-driven magnetic ordering transition, where INS data indicate the closing of a spin gap, but in the presence of a nondiverging correlation length [11]. Since it is known that $La_{2-x}Sr_xCuO_4$ shows spatially disordered charge stripes [49], which in turn lead to modulated magnetic couplings, our modeling of random-mass disorder can be expected to qualitatively describe the soft-mode behavior of $La_{2-x}Sr_xCuO_4$. Therefore, we propose that quenched disorder tends to localize low-energy magnetic modes at the QPT in $La_{2-x}Sr_xCuO_4$, thus providing a cutoff to the apparent magnetic correlation length. Disorder is also expected to cut off one-parameter scaling in $\chi''(\omega, T)$—this is testable in future experiments.

Summary.—For coupled-dimer magnets, we have proposed an efficient method to calculate real-frequency excitation spectra in the presence of bond randomness across the entire phase diagram. This allows one in particular to study magnetic excitations near quantum criticality, where the effect of disorder is generically strong. Using the bilayer Heisenberg model as an example, we have studied disorder-induced spectral weight transfer and weak magnetic order. We find strong broadening of low-energy excitation spectra due the localization tendency of the relevant modes. Further high-resolution INS experiments, e.g., on $Tl_{1-x}K_xCuCl_3$ [39], which could test our predictions are called for.

Our method can be extended to the case with magnetic field, in order to access excitations of disordered magnon Bose condensates, Bose glasses, or disordered supersolids. A generalization to frustrated dimer lattices and to incommensurate order is possible as well.

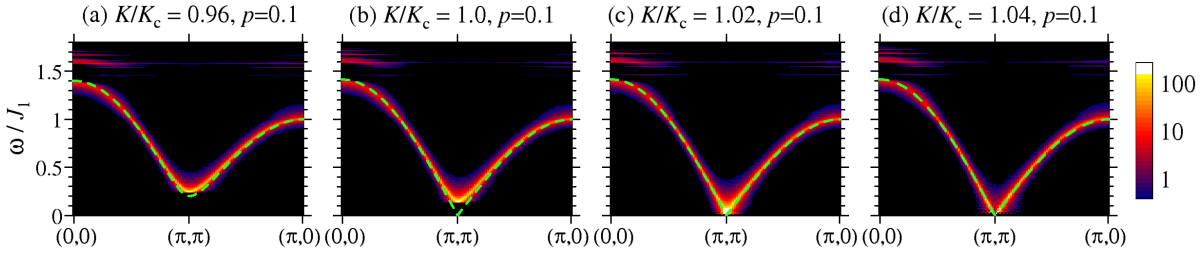

FIG. 5 (color online). Results for the susceptibility $\chi''(\vec{q}, \omega)$ as in Fig. 1, but for a density of p *strong* intradimer couplings with $J_2 = 3J_1/2$.

I thank E. Andrade, S. Burdin, J. Chang, R. Doretto, D. Joshi, M. Müller, C. Rüegg, and S. Wessel for discussions. This research was supported by the DFG through FOR 960 and GRK 1621. In addition, financial support by the Heinrich-Hertz-Stiftung NRW and the hospitality of the Centro Atomico Bariloche during early stages of this project are gratefully acknowledged.

[1] S. Sachdev, *Quantum Phase Transitions* (Cambridge University Press, Cambridge, England, 2010), 2nd ed.
[2] S. Sachdev, Nat. Phys. **4**, 173 (2008).
[3] T. Giamarchi, C. Rüegg, and O. Tchernyshyov, Nat. Phys. **4**, 198 (2008).
[4] H. von Löhneysen, A. Rosch, M. Vojta, and P. Wölfle, Rev. Mod. Phys. **79**, 1015 (2007).
[5] T. Vojta, J. Phys. A **39**, R143 (2006) and references therein.
[6] T. Vojta, J. Low Temp. Phys. **161**, 299 (2010).
[7] R. B. Griffiths, Phys. Rev. Lett. **23**, 17 (1969).
[8] C. Rüegg, A. Furrer, D. Sheptyakov, T. Strässle, K. W. Krämer, H.-U. Güdel, and L. Melesi, Phys. Rev. Lett. **93**, 257201 (2004).
[9] B. Lake, D. A. Tennant, C. D. Frost, and S. E. Nagler, Nat. Mater. **4**, 329 (2005).
[10] C. Rüegg, B. Normand, M. Matsumoto, A. Furrer, D. F. McMorrow, K. W. Krämer, H.-U. Güdel, S. N. Gvasaliya, H. Mutka, and M. Boehm, Phys. Rev. Lett. **100**, 205701 (2008).
[11] J. Chang, N. B. Christensen, C. Niedermayer, K. Lefmann, H. M. Rønnow, D. F. McMorrow, A. Schneidewind, P. Link, A. Hiess, M. Boehm, R. Mottl, S. Pailhes, N. Momono, M. Oda, M. Ido, and J. Mesot, Phys. Rev. Lett. **102**, 177006 (2009).
[12] M. B. Stone, A. Podlesnyak, G. Ehlers, A. Huq, E. C. Samulon, M. C. Shapiro, and I. R. Fisher, J. Phys. Condens. Matter **23**, 416003 (2011).
[13] D. Hüvonen, S. Zhao, M. Månsson, T. Yankova, E. Ressouche, C. Niedermayer, M. Laver, S. N. Gvasaliya, and A. Zheludev, Phys. Rev. B **85**, 100410 (2012).
[14] D. Hüvonen, S. Zhao, G. Ehlers, M. Månsson, S. N. Gvasaliya, and A. Zheludev, Phys. Rev. B **86**, 214408 (2012).
[15] B. Nafradi, T. Keller, H. Manaka, U. Stuhr, A. Zheludev, and B. Keimer, Phys. Rev. B **87**, 020408(R) (2013).
[16] S. Sachdev and R. N. Bhatt, Phys. Rev. B **41**, 9323 (1990).
[17] T. Matsuda and K. Hida, J. Phys. Soc. Jpn. **59**, 2223 (1990); K. Hida, *ibid.* **59**, 2230 (1990).
[18] K. Hida, J. Phys. Soc. Jpn. **61**, 1013 (1992).
[19] A. W. Sandvik and D. J. Scalapino, Phys. Rev. Lett. **72**, 2777 (1994).
[20] A. V. Chubukov and D. K. Morr, Phys. Rev. B **52**, 3521 (1995).
[21] V. N. Kotov, O. Sushkov, Zheng Weihong, and J. Oitmaa, Phys. Rev. Lett. **80**, 5790 (1998).
[22] L. Wang, K. S. D. Beach, and A. W. Sandvik, Phys. Rev. B **73**, 014431 (2006).
[23] K. Takatsu, W. Shiramura, and H. Tanaka, J. Phys. Soc. Jpn. **66**, 1611 (1997).
[24] A. Oosawa, M. Ishii, and H. Tanaka, J. Phys. Condens. Matter **11**, 265 (1999).
[25] Ch. Rüegg, N. Cavadini, A. Furrer, H.-U. Güdel, K. Krämer, H. Mutka, A. Wildes, K. Habicht, and P. Vorderwisch, Nature (London) **423**, 62 (2003).
[26] M. Matsumoto, B. Normand, T. M. Rice, and M. Sigrist, Phys. Rev. Lett. **89**, 077203 (2002).
[27] Y. Sasago, K. Uchinokura, A. Zheludev, and G. Shirane, Phys. Rev. B **55**, 8357 (1997).
[28] M. Jaime, V. F. Correa, N. Harrison, C. D. Batista, N. Kawashima, Y. Kazuma, G. A. Jorge, R. Stern, I. Heinmaa, S. A. Zvyagin, Y. Sasago, and K. Uchinokura, Phys. Rev. Lett. **93**, 087203 (2004).
[29] S. E. Sebastian, N. Harrison, C. D. Batista, L. Balicas, M. Jaime, P. A. Sharma, N. Kawashima, and I. R. Fisher, Nature (London) **441**, 617 (2006).
[30] T. Sommer, M. Vojta, and K. W. Becker, Eur. Phys. J. B **23**, 329 (2001).
[31] An approach similar to that in Ref. [30] has been developed independently in J. Romhanyi, K. Totsuka, and K. Penc, Phys. Rev. B **83**, 024413 (2011).
[32] See Supplemental Material at http://link.aps.org/supplemental/10.1103/PhysRevLett.111.097202 for a description of our numerical approach, additional results for the spectra and localization properties, and a brief discussion of previous work on excitations in disordered magnets.
[33] M. Vojta and T. Ulbricht, Phys. Rev. Lett. **93**, 127002 (2004).
[34] D. Joshi and M. Vojta (to be published).
[35] R. Eder, Phys. Rev. B **57**, 12832 (1998).
[36] A. B. Harris, J. Phys. C **7**, 1671 (1974).
[37] R. Sknepnek, T. Vojta, and M. Vojta, Phys. Rev. Lett. **93**, 097201 (2004).
[38] Y.-C. Lin, H. Rieger, N. Laflorencie, and F. Igloi, Phys. Rev. B **74**, 024427 (2006).
[39] A. Oosawa and H. Tanaka, Phys. Rev. B **65**, 184437 (2002).
[40] R. A. Cowley and W. J. L. Buyers, Rev. Mod. Phys. **44**, 406 (1972).
[41] S. E. Nagler, W. J. L. Buyers, R. L. Armstrong, and R. A. Ritchie, J. Phys. C **17**, 4819 (1984).
[42] Y. J. Uemura and R. J. Birgeneau, Phys. Rev. B **36**, 7024 (1987).
[43] A. L. Chernyshev, Y. C. Chen, and A. H. Castro Neto, Phys. Rev. B **65**, 104407 (2002).
[44] E. R. Mucciolo, A. H. Castro Neto, and C. Chamon, Phys. Rev. B **69**, 214424 (2004).
[45] A. Chakraborty and G. Bouzerar, Phys. Rev. B **81**, 172406 (2010).
[46] A. L. Chernyshev, M. E. Zhitomirsky, N. Martin, and L.-P. Regnault, Phys. Rev. Lett. **109**, 097201 (2012).
[47] G. Xu, G. Aeppli, M. E. Bisher, C. Broholm, J. F. DiTusa, C. D. Frost, T. Ito, K. Oka, R. L. Paul, H. Takagi, and M. M. J. Treacy, Science **289**, 419 (2000).
[48] S. Haravifard, S. R. Dunsiger, S. El Shawish, B. D. Gaulin, H. A. Dabkowska, M. T. F. Telling, T. G. Perring, and J. Bonca, Phys. Rev. Lett. **97**, 247206 (2006).
[49] M. Vojta, Adv. Phys. **58**, 699 (2009).